AIAA 80-1825R

Advanced Circulation Control Wing System for Navy STOL Aircraft

James H. Nichols Jr.* and Robert J. Englar†
David W. Taylor Naval Ship Research and Development Center, Bethesda, Md.

An advanced high lift system is being developed which combines a circulation control wing (CCW) with upper surface blowing (USB) to produce significant lift for STOL operations by Navy aircraft. The concept uses circulation control (CC) to pneumatically deflect USB engine thrust and thus augment aerodynamic wing lift produced by the outboard CCW. Wind tunnel investigations have confirmed significant thrust turning to angles near 165 deg, providing a simple, highly effective STOL and thrust reverser system. A no-moving-parts VTOL system obtained by deflecting thrust to angles around 90 deg is also suggested. The paper presents experimental results, a conceptual design for a proposed CCW + CC/USB STOL aircraft, and predicted STOL characteristics for that aircraft. Payoff in aircraft mechanical simplicity is also discussed.

Introduction

THE circulation control wing (CCW) concept is a mechanically simple high lift system which employs tangential blowing over a rounded trailing edge to yield very high lift augmentation with an expenditure of minimum amounts of jet momentum and mass flow.[1,2] The system has been under development since 1970 at David W. Taylor Naval Ship Research and Development Center (DTNSRDC), where the basic concept was developed. A configuration for proof-of-concept flight test was designed and experimentally evaluated for application to a Navy/Grumman A-6A aircraft,[3] as shown in Fig. 1. The rounded CCW trailing edge is visible, as are air supply lines, externally mounted for simplicity, carrying engine bleed air to the CCW. These flight investigations conducted by Grumman confirmed the DTNSRDC tunnel predictions that CCW could double aircraft lifting capabilities using only bleed air available from the existing engines. Flight speeds as low as 67 knots were demonstrated even though blown $C_{L_{\max}}$ and V_{stall} were not achieved owing to control power limitations. Test results are published in Refs. 4-6. A summary of A-6/CCW STOL performance relative to the conventional A-6A aircraft is given in Fig. 2, showing the CCW as a viable system for providing STOL potential for high performance Navy aircraft.

The mechanical simplicity and high lift augmentation of CCW are quite attractive from a weight and STOL performance standpoint. Furthermore, it was envisioned that certain characteristics of the system would be quite compatible with the already proven (YC-14, QSRA, etc.) upper surface blowing (USB) system. Maximum lift coefficients for the A-6/CCW aircraft (aspect ratio 5.3) and a typical four-engine USB configuration (aspect ratio 7.5) with cruise-typical D-shaped nozzles[7] are shown in Fig. 3. For USB, the incremental lift due to deflecting thrust is made up of the vertical component of the deflected engine thrust, C_T sin $(\delta_j + \alpha)$, with a contribution due to thrust induced circulation lift, C_{L_Γ}. For CCW,[3] the increment of lift above that due to camber and incidence is all blowing-induced circulation lift, with virtually no vertical thrust component. By taking advantage of the ability of the circulation control phenomenon to entrain and control the engine thrust direction, as shown in Fig. 4, the USB mechanical flap system and its supporting structure and actuators can be eliminated and replaced by the CCW round trailing edge and internal blowing plenum. For the USB/flap system, thrust deflection angle θ is controlled by increasing flap deflection until jet separation occurs. For the CC/USB system, θ depends on the CCW plenum pressure, slot mass flow, and the flow entrainment effects of the CCW trailing edge. That is, θ is changed nearly instantly by a flow control valve or pressure regulator. The thrust can be deflected to angles up to 165 deg, thereby providing a

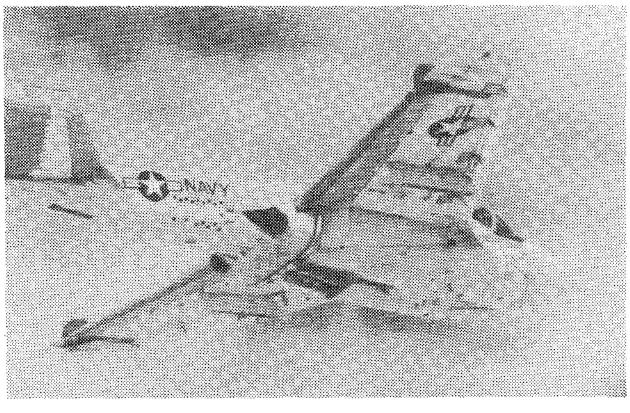

Fig. 1 A-6/CCW flight demonstrator aircraft.

BASED ON FLIGHT DEMONSTRATION RESULTS TOGW 35,700 LB., LGW 33,000 LB. CORRECTED TO SEA LEVEL, STANDARD DAY	A-6 (30° FLAPS)	A-6/CCW
85% INCREASE IN $C_{L_{MAX}}$	2.1	3.9 (C_μ = 0.30)
35% REDUCTION IN POWER-ON APPROACH SPEED	118 KTS (C_L = 1.49)	76 KTS (0.75 P_{MAX}, C_μ = 0.14, C_L = 2.78)
65% REDUCTION IN LANDING GROUND ROLL	2450 FT	900 FT
30% REDUCTION IN LIFT OFF SPEED	120 KTS (C_L = 1.41)	82 KTS (0.6 P_{MAX}, C_μ = 0.04, C_L = 2.16)
60% REDUCTION IN TAKEOFF GROUND ROLL	1450 FT	600 FT
75% INCREASE IN PAYLOAD/FUEL AT TYPICAL OPERATING WEIGHT (EW ≈ 28,000 LB.)	45,000 LB.	58,000 LB.

Fig. 2 A-6/CCW STOL performance.

Presented as Paper 80-1825 at the AIAA Aircraft Systems and Technology Meeting, Anaheim, Calif., Aug. 4-6, 1980; submitted Sept. 10, 1980; revision received May 29, 1981. This paper is declared a work of the U.S. Government and therefore is in the public domain.

*Head, Aircraft Division, STOL Aerodynamics Group. Member AIAA.
†CCW Program Manager, STOL Aerodynamics Group, Aircraft Division. Member AIAA.

pneumatic thrust reverser or providing a vertical thrust deflection offering the possibility of VTOL flight, in addition to STOL operation for $\theta < 90$ deg.

The key to achieving the payoffs of a combined CC/USB is the thrust-deflecting capability of the CC trailing edge, and any limitations placed on that ability by engine thrust levels, nozzle geometry, and freestream dynamic pressure. To address these questions, static and freestream investigations were conducted to provide a general data base to assess STOL performance potential of an aircraft designed around a CCW + CC/USB high lift system.

Experimental Investigations

Model

The investigation presented herein was intended to evaluate CC/USB thrust-turning capability and made use of an existing generic half-span model that had been used to evaluate CCW and USB systems independently.[8] This model, shown mounted in the DTNSRDC 8- × 10-ft subsonic tunnel in Fig. 5, was a combination of an existing $\mathcal{R} = 4$ CCW wing section and a USB propulsion simulator, and as such is referred to as the CCW/USB configuration. This engine simulator employs two 5.5-in.-diam tip-turbine fans mounted in tandem to generate an output pressure ratio typical of existing turbofan engines. A D-nozzle is shown in the figure, where a simulated internal nozzle flap produced a width/height ratio of 3.3 at the exit.

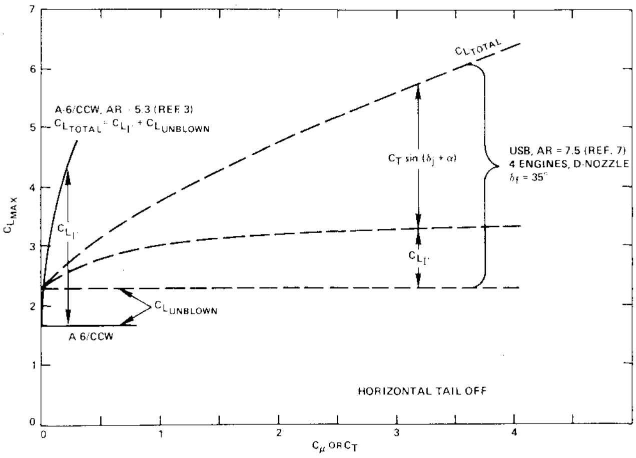

Fig. 3 Maximum lift coefficients for typical CCW and USB aircraft configurations.

As assembled, the model does not properly represent a typical CC/USB configuration. First, a single CCW plenum runs the entire wing span (thus the CCW/USB designation), which uses more mass flow than necessary and generates blowing-induced circulation lift that cannot be mathematically separated from thrust-induced lift except during static conditions when the circulation lift is zero. Second, the engine may be oversized relative to the wing. Third, the aspect ratio of 4.0 is lower than that planned for the aircraft/mission to be addressed in this paper.

The airfoil is a 14% thick supercritical section with a 15% chord Krueger leading-edge flap deflected to 40 deg. CCW trailing-edge parameters are based on the A-6/CCW development[3]: a radius-to-chord ratio of 0.036 and a local slot height-to-radius ratio of 0.031. Measured slot height varied nearly linearly with plenum pressure (P_{T_D}), with a slot area increase of 17% occurring at a maximum plenum pressure of 120 in. Hg (58.9 psig). The model was mounted on the tunnel balance frame independent of a splitter plate and simulated fuselage in order to remove the wing from the tunnel boundary layer, simulate fuselage interference, and allow the wing and engine to be isolated.

The experiments were conducted in three steps: 1) a static bench test for flow visualization, 2) a static wind tunnel test to quantify thrust turning, and 3) a wind-on test to quantify thrust turning during simulated in-flight and landing conditions. The effects of higher thrust levels, variations in angle of attack, operation in ground effect, and a configuration buildup to determine individual contributions of CCW and USB alone were investigated during the third phase.

Flow Visualization Results

Prior to the tunnel installation, a static bench test was conducted using flow visualization for a preliminary indication of thrust deflecting capability of the model. A

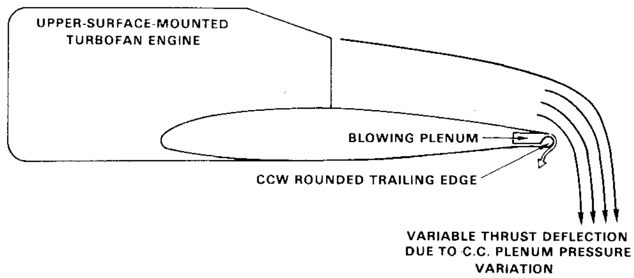

Fig. 4 CC/USB engine thrust deflector.

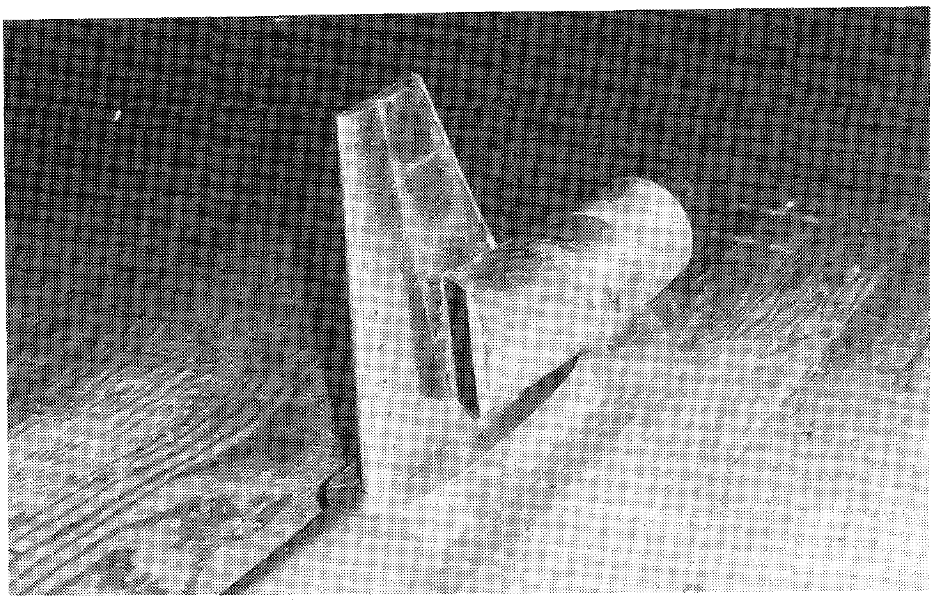

Fig. 5 Half-span CCW/USB model.

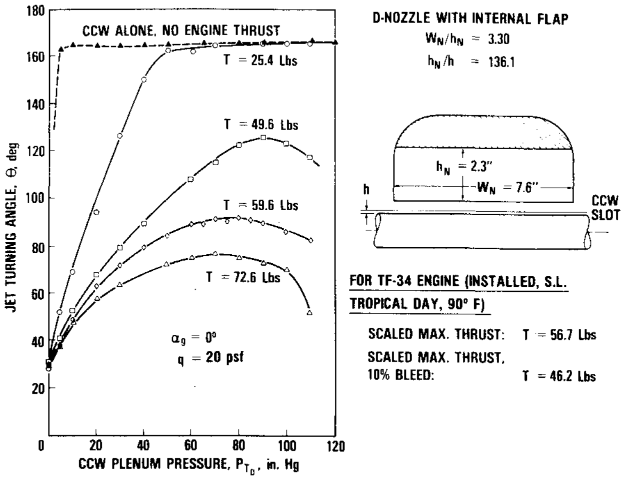

Fig. 6 CCW/USB static thrust turning.

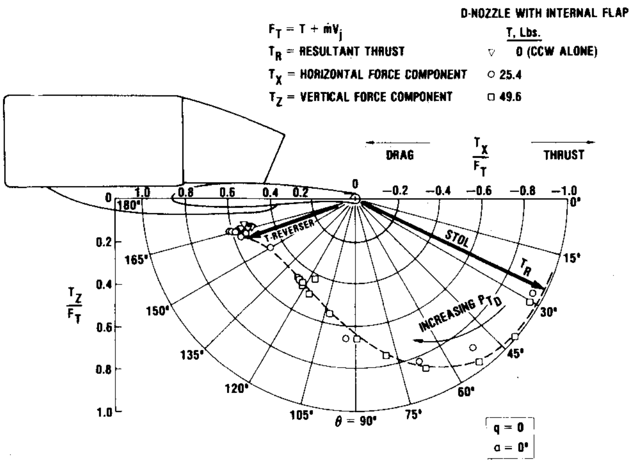

Fig. 7 CCW/USB turning angle and thrust recovery efficiency.

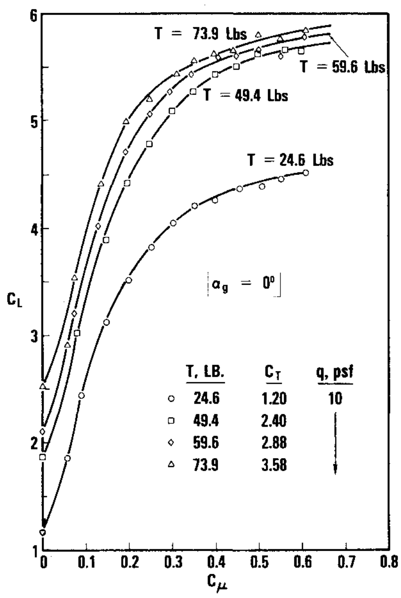

Fig. 8 Effect of blowing and thrust variation on CCW/USB lift coefficient.

movable tuft was located throughout the nozzle exit, and the main jet sheet appeared to turn substantially around the trailing edge when CC blowing was applied.

Static Thrust Turning Results

Several exhaust nozzles ranging from round to higher aspect ratio (width/height) D-nozzles were evaluated statically (no freestream) to determine the best nozzle in terms of jet turning. Jet turning was greatly improved when either the jet was spread wider and closer to the wing surface and CCW slot, or when the jet height was reduced relative to the CCW slot height. The round nozzles produced relatively little turning because of their large jet height and low aspect ratio of 1.0. The greatest turning performance was provided by the D-nozzle with internal flap shown in Fig. 5. Turning performance of this aspect ratio 3.3 nozzle is shown in Fig. 6 where the jet-turning angle is determined by resolution of measured horizontal and vertical force components. Static CCW jet turning (no engine thrust) is shown as the dashed curve, with 165 deg achieved above a plenum pressure of 5 in. Hg (2.46 psig). This represents an upper limit on propulsive jet turning. For a moderate level of thrust of 25.4 lb (calibrated at the nozzle exit with $P_{T_D} = 0$), turning increases with increased plenum pressure until at 50 in. Hg the propulsive jet is turned to nearly the same angle as the CCW jet alone. At higher thrust levels, less turning occurs owing to the higher thrust kinetic energy levels, which are more difficult to entrain and deflect. Maximum thrust values for a turbofan engine with an exhaust pressure ratio of about 1.5, both with and without core bleed to provide the plenum pressure, are shown for comparison scaled to the model engine. These scaled values are from full-scale TF-34 installed thrust for sea-level tropical day (90°F) conditions with a 60-knot vehicle speed. Jet turning of at least 95 deg can be achieved at maximum thrust, with values ranging up to 165 deg at lower thrust levels. This amount of jet turning clearly provides ample thrust deflection for STOL takeoff and approach operation, as well as for reversed thrust upon landing. Also implied is the possibility of a no-moving-parts VTOL system where static thrust deflection of 85-95 deg can provide vertical lifting and control capability. These thrust-turning capabilities and associated thrust recovery are shown in Fig. 7. Here, F_T is the sum of the calibrated engine thrust (no turning) plus the measured jet momentum at the CCW slot exit, and thus includes all energy input to the system. The length of the vector T_R represents effective thrust recovery and its direction is the turning angle θ. For STOL operation (say $\theta \leq 60$ deg) more than 90% of the input energy is recovered, while as a thrust reverser, 55-60% of the thrust is reversed through 165 deg.

Static data were taken in the presence of a fixed groundboard. At a groundboard height-to-wing-chord ratio of 1, no significant change in static turning relative to data taken out of ground effect occurred.

Wind-On Thrust-Turning Results

Data were taken in a freestream to find any degradation of thrust turning due to dynamic pressure (q), and to determine aerodynamic forces on the system. In Fig. 8, the lift coefficient for constant thrust values is plotted against the momentum coefficient C_μ, defined as nondimensionalized slot momentum, $\dot{m}V_j/qS$. Here, even though static thrust turning is less at higher thrust levels, increased thrust yields a larger vertical component and thus higher total C_L; values of nearly 6 are generated at $\alpha = 0$ deg.

Optimum CCW + CC/USB operation will occur with the outboard CCW slot and the inboard CC/USB thrust-deflecting slot operating independently at different blowing conditions. Since a single plenum is used on the model, the outboard CCW and the inboard CC/USB can only be operated simultaneously and at the same pressures. Thus C_μ is the total momentum coefficient for the entire wing span rather than for the CC/USB system. Based on A-6/CCW experience, a maximum value of 0.30 on total C_μ is reasonable for the near term. Results at a tunnel dynamic pressure of 10 psf (approximately 55 knots freestream velocity) are presented in Fig. 8. These are appropriate since

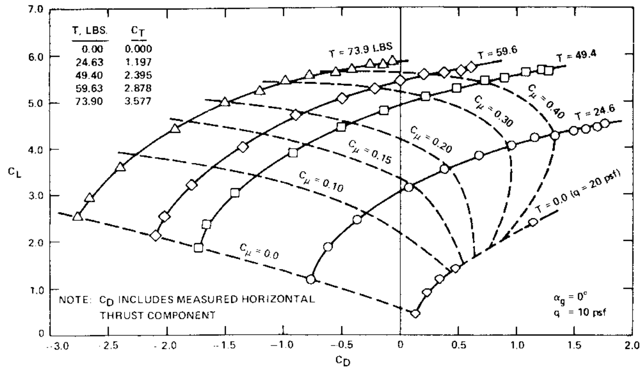

Fig. 9 Drag polars for CCW/USB configuration at $q = 10$ psf and $\alpha_g = 0$ deg.

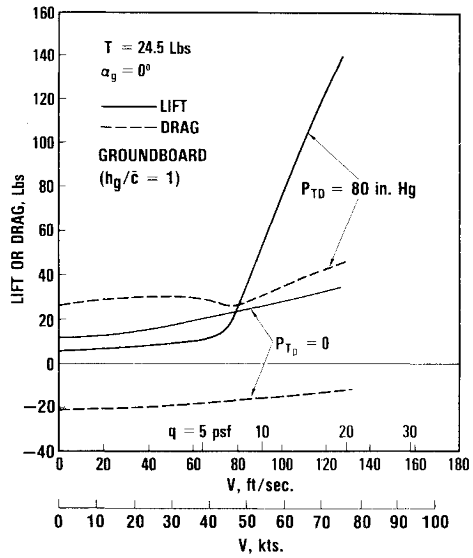

Fig. 10 CCW/USB simulated thrust reverser.

approach and liftoff speeds for anticipated aircraft configurations and weights are in the range 50-60 knots. The corresponding drag polars are presented in Fig. 9 as curves of constant thrust or C_μ, where the term C_D includes the measured horizontal thrust component. A total drag value of 0, which is required for an equilibrium landing approach, corresponds to available C_L of almost 6 at $\alpha = 0$ deg, while negative drag values at high C_L imply availability of excess thrust for takeoff and climb at high lift.

Simulated Thrust Reverser

The addition of a simple thrust reverser to a powered lift STOL aircraft can further reduce the already short landing distance provided by low touchdown velocities and reduced kinetic energy. An effective thrust reverser must provide maximum thrust turning, quick response after touchdown, reduction in lift to increase weight on the wheels to improve braking efficiency, and mechanical simplicity. The CCW/USB model was used to simulate landing ground rolls at 0 deg incidence with a fixed groundboard located at 1.0 $\bar{c}$ below the model center of gravity. These simulated ground rolls were conducted at constant thrust and plenum pressure by taking data at discrete freestream velocities as the tunnel dynamic pressure was reduced by steps from 20 to 0 psf. The results indicate the maximum turning possible for the conditions simulated, since they are steady-state. Again, the outboard blowing slot can not be turned off and thus undesired outboard CCW wing lift continues to be generated during ground roll.

Figure 10 depicts resulting forces generated by a calibrated thrust of 24.5 lb with plenum pressures of 0 and 80 in. Hg. The terms lift and drag here are synonymous with measured vertical and horizontal forces at $\alpha = 0$ deg along the runway, including the corresponding components of thrust. Thus, with blowing-off ($P_{T_D} = 0$), thrust recovery (or negative drag) increases as the aerodynamic drag decays with dynamic pressure. At zero velocity, almost 90% of the initial thrust is recovered as a forward horizontal force, with a vertical component of nearly 50% resulting from a downward deflection of about 30 deg due to the USB nozzle/wing arrangement (see Fig. 6). With a plenum pressure of 80 in. Hg applied, drag remains positive, directed aft over the entire speed range owing to increased jet turning. The remaining lift at low velocity is about half the value at $P_{T_D} = 0$, thus providing improved braking force. At zero velocity, these force components with blowing-on include approximately 10.2 lb of drag and 2.7 lb of lift due to the reaction force of the CCW jet momentum alone. Turning off the outboard CCW plenum would reduce these values by roughly half, resulting in a net drag of 86% of the input engine thrust and a lift of only 10% of this thrust.

The resultant force-turning angles from the thrust reverser simulation are shown in Fig. 11 for thrust settings of 24.5 and

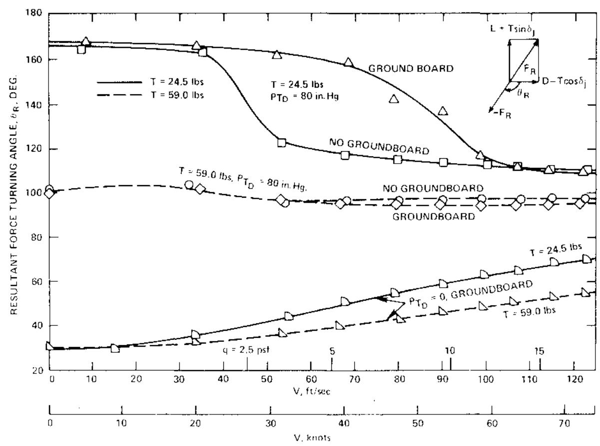

Fig. 11 CCW/USB simulated thrust reverser resultant force turning, $\alpha_g = 0$ deg.

59.0 lb and blowing pressures of 0 and 80 in. Hg, both with and without a fixed groundboard. Here, the resultant force angle θ_R is defined as [180 deg-arctan (vertical force/horizontal force)]. This angle θ_R is similar to θ in Fig. 6, except it now includes outboard CCW aerodynamic forces which are not easily separated from inboard thrust components when a freestream is present. At zero velocity, $\theta = \theta_R$ and the resultant force F_R equals the sum of the thrust and jet momentum components only. For a thrust of 24.5 lb with blowing in ground effect, force turning rapidly rises from 110 to 165 deg as speed decreases below the touchdown value of about 55 knots. Without a groundboard, that rise does not occur until speed decreases to about 25-30 knots. An aircraft near touchdown would probably always fly on the favorable ground effect curve; speeds of less than 50 knots are not likely prior to the landing ground roll. For a thrust of 59 lb with blowing, the turning angle is somewhat less than above, but almost constant with decreasing velocity and with much less dependency on ground effect. For no blowing, both thrust levels decay to the configuration's initial blowing-off angle of 30 deg. It appears that thrust reversal is quite responsive to both thrust and blowing levels and that a simple no-moving-parts system is feasible.

Configuration Development

The above data indicate the CC/USB no-moving-parts thrust-deflection concept can provide a simple light-weight

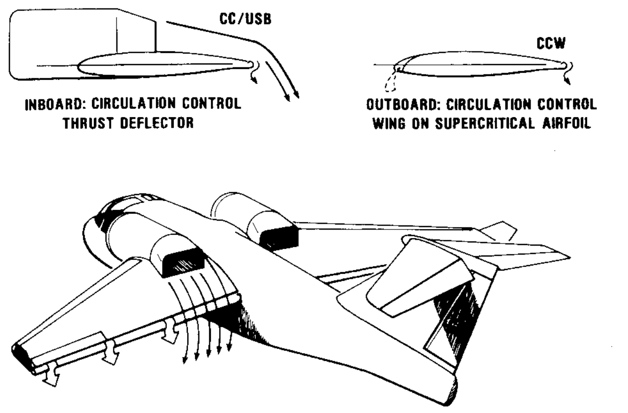

Fig. 12 Proposed CCW + CC/USB STOL aircraft.

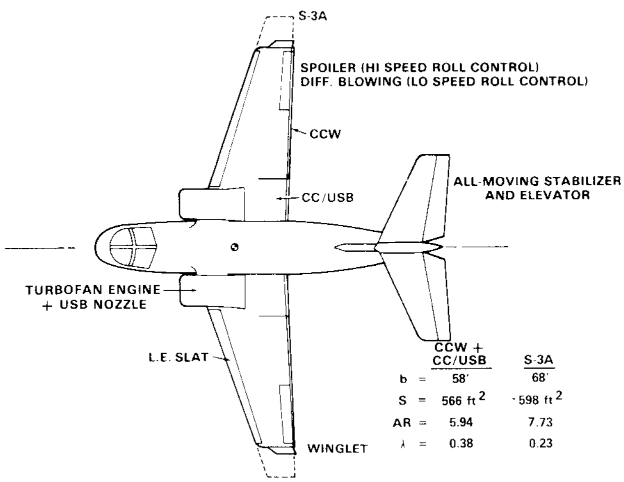

Fig. 13 Proposed CCW + CC/USB STOL aircraft planform.

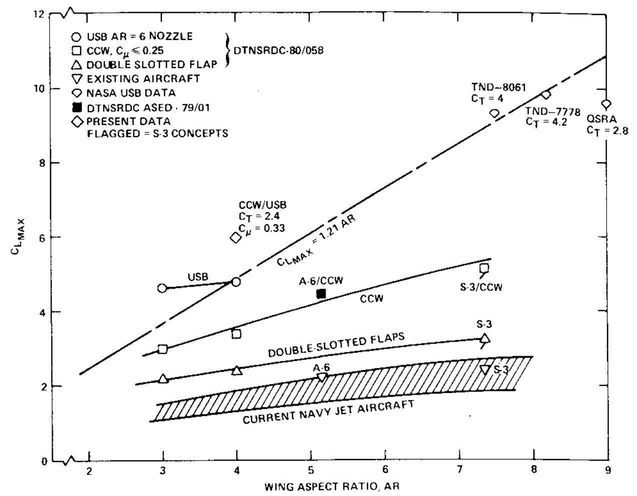

Fig. 14 $C_{L_{\max}}$ variation with aspect ratio.

replacement for large mechanical USB/flap systems, and can provide effective thrust reversing with no additional components required. Present USB aircraft like the YC-14 and QSRA combine the inboard USB engine/mechanical flap system with double-slotted mechanical flaps outboard to provide the required lift for takeoff. Replacement of these flaps and outboard drooped or blown ailerons with a CCW trailing edge eliminates the mechanical complexity by allowing transition from the high lift to cruise configuration by terminating blowing. Applied to a relatively thick trailing-edge supercritical airfoil, a small-radius CCW trailing-edge surface can remain fixed at relatively little, if any, penalty in cruise drag. To evaluate both the drag and lift-augmenting capabilities of small trailing-edge radius CCW configurations, a two-dimensional wind tunnel evaluation of a typical NASA supercritical airfoil[9] with a CCW radius 25% that of the A-6/CCW airfoil has been completed at DTNSRDC. Results[10] for this small trailing-edge CCW airfoil confirm lift generation comparable to the A-6/CCW airfoil, and unblown drag levels essentially the same as the baseline bluff supercritical airfoil.

A subsonic cruise STOL aircraft using the above concepts is postulated as the configuration shown in Figs. 12 and 13. To provide timely STOL capability without development of a completely new aircraft, the proposed configuration makes maximum use of existing Lockheed S-3A aircraft components, namely, the airframe, wing primary structure, engines, and as much of the control surfaces as feasible. A supercritical wing with a small radius CCW trailing-edge running full span will be installed. The two pylon-mounted TF-34 engines will be moved to the wing upper surface near the fuselage junction. Engine relocation provides the CC/USB thrust-turning system, minimizes one-engine-out yawing moments, and reduces air supply crossover duct lengths required for controlled flight with one engine out. Two plenums are provided in each wing half. The inboard plenum supplies higher pressure air from TF-34 core bleed for USB thrust deflection. The outboard plenum supplies lower pressure TF-34 fan air to supply the CCW trailing edge. This multisource air supply system using turbofan core and fan bleed air simultaneously has already been successfully employed on the QSRA aircraft.[11] The inboard and outboard plenums are independently controlled using separate flow valves.

The existing S-3A wing aspect ratio of 7.73 may be retained, or as Fig. 13 shows, the removal of 5 ft from each wing tip to reduce the span to 58 ft and $\mathcal{R}$ to about 6 will provide additional flight deck clearance on smaller air-capable ships. The winglets shown may be used to regain effective aspect ratio in cruise, to carry spanwise high lift distribution closer to the tip, or as a directional control device at low speed. Proposed roll control is by deflecting the existing spoilers at high speed, and by differential CCW blowing between left and right wing[12] at low speeds. Longitudinal tail location and configuration were not investigated in the present tests. The high T-tail with elevator is shown as being typical of other USB aircraft. However, tail-off pitching moments of the CCW/USB model were similar to those of the A-6/CCW (Ref. 3) at the same lift coefficient. The A-6/CCW pitching moments were trimmed by a low-mounted all-moving stabilator which benefitted from the additional dynamic pressure and downwash available from the flowfield of the engine exhaust. Further investigations are planned to examine longitudinal trim requirements and tail arrangement.

STOL Performance Predictions

To predict STOL performance of the proposed CCW + CC/USB aircraft, the existing data must be adjusted to account for the difference in aspect ratio between the model and proposed aircraft. The effect of aspect ratio on $C_{L_{\max}}$ is presented in Fig. 14 for a family of current Navy jet aircraft, for a series of DTNSRDC high lift model data[8] at low aspect ratios of 3 and 4, for existing aircraft with proposed high lift systems, and for several USB configurations. At $\mathcal{R} = 4$, a lift increment of approximately 1.5 results from adding the CCW/USB concept to the USB-alone configuration. Adding that same increment to the typical higher aspect ratio USB configurations shown results in a $C_{L_{\max}}$ greater than 10 for the proposed CCW + CC/USB aircraft of Figs. 12 and 13 with $\mathcal{R} = 7.73$, $C_T = 2.4$, and $C_\mu = 0.33$.

To predict estimated lift and drag data for the S-3A based CCW + CC/USB aircraft within these suggested limits, a

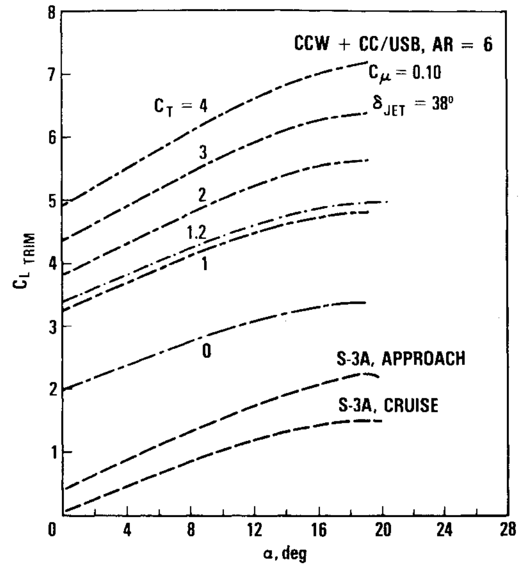

Fig. 15 High lift capability of conventional S-3A and proposed CCW + CC/USB aircraft.

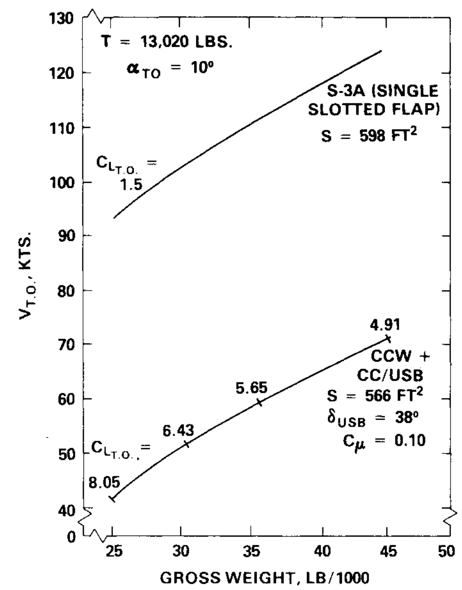

Fig. 16 Comparative liftoff velocities, sea-level tropical day.

more conservative method was used. Figure 15 shows the resulting lift curves for the $\text{Æ}=6$ configuration. Existing two-engine USB data[13] for incremental lift due to C_T and jet deflection of 38 deg were adjusted to the proposed configuration wing geometry. These data were added to lift curves previously developed by Lockheed for an S-3A/CCW configuration using $C_\mu=0.10$ (here labeled $C_T=0$). A $C_{L_{max}}$ of 6 at $C_T=2.4$ and $C_\mu=0.10$ is obtained, which is conservative compared to a value of about 7 obtained by extrapolating data to $\text{Æ}=6.0$ at the same C_μ and C_T. This is probably due to actual thrust deflection angles greater than the 38 deg assumed. Even if these conservative data are used to predict STOL performance, some very promising potential appears, as follows.

All STOL performance to be discussed below is based on sea-level tropical day (90°F) conditions with standard S-3/TF-34 maximum installed thrust of 13,020 lb total. Losses due to engine thrust droop, bleed, and velocity of 60 knots are included. The proposed $\text{Æ}=6$ configuration is compared in Fig. 16 with the conventional S-3A with $\text{Æ}=7.73$ in terms of liftoff velocity. For a takeoff gross weight range of 35,000-40,000 lb, conventional liftoff speeds of 115 knots can be reduced to 60-65 knots. The implications on reduced requirements for catapult equipment (if in fact any is required at all) are significant. The resulting short noncatapulted takeoff distances are compared in Fig. 17 for wind-over-deck (WOD) velocities of 0 and 20 knots. Here, the takeoff procedure for the proposed aircraft is to accelerate at maximum thrust (bleed-off and no-thrust deflection) until the rotation speed is reached. At rotation, blowing is initiated and instantaneous thrust deflection and lift augmentation occur. This procedure was successfully and comfortably used by Grumman test pilots with the A-6/CCW.[5,6] Conventional S-3 takeoff rolls of 1175-1650 ft are reduced to 200-325 ft for a 20-knot WOD. Takeoff distances of 450-650 ft are possible if no wind over deck is available. For both conventional and CCW + CC/USB aircraft, the installed thrust-to-weight ratios range from 0.38 to 0.33. These are twin-engine performance predictions; analysis of takeoff and control with one engine inoperative is now being conducted.

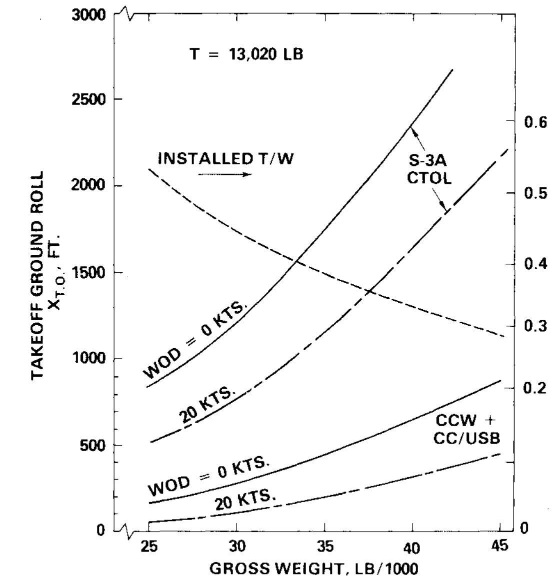

Fig. 17 Comparative unassisted takeoff ground rolls, sea-level tropical day.

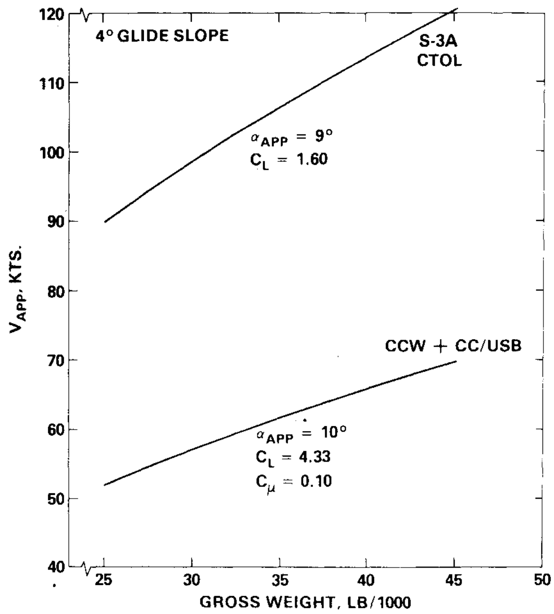

Fig. 18 Equilibrium approach speeds, sea-level tropical day.

Figure 18 compares equilibrium approach speeds at an angle of attack of 9 or 10 deg and on a 4-deg glide slope. Since

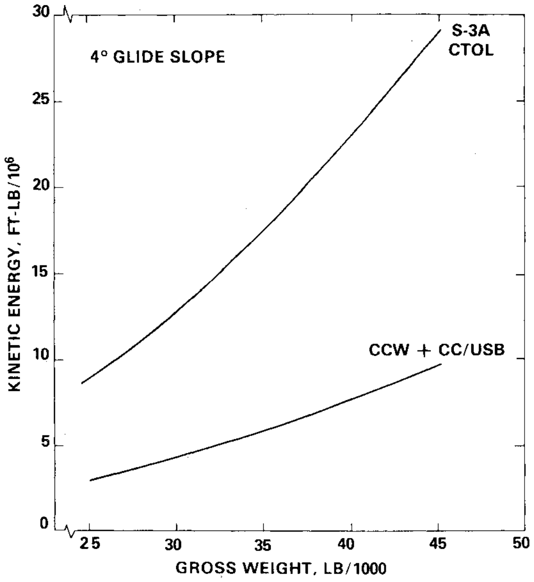

Fig. 19 Kinetic energy at equilibrium touchdown speed, sea-level tropical day.

no flare is used in Navy approaches, this glide slope is constant and forces must be in equilibrium along that flight path. This requires additional drag generation for USB aircraft, since high lift is achieved at high thrust settings which result in high thrust recovery. This thrust recovery is offset for the CCW + CC/USB aircraft by the induced drag generated by CCW. Thus all approaches are made along the $C_D = 0$ axis of Fig. 9 but at the appropriate approach angle of attack of 10 deg. For a landing weight of 30,000-35,000 lb, the approach speed is reduced from 95 to 55 knots by the CCW + CC/USB. For a fixed bleed rate from the engines, available C_μ will not remain constant with gross weight as shown in Figs. 16 and 18, but will increase as weight decreases. Thus the actual speeds attainable by the proposed aircraft at lighter weights will be less than those shown if sufficient control power is provided. The reduction in kinetic energy is shown in Fig. 19 at touchdown speeds associated with the above approach conditions. The 70% reductions in kinetic energy indicate proportional reductions in landing ground rolls, plus the associated increases in system lift. With the proposed CC/USB thrust reverser, there is a strong possibility for reducing or eliminating arresting gear. These lower approach speeds also imply an improved steeper glide slope to minimize flight through carrier-induced turbulence, increased pilot visibility from approach at lower incidences, and increased pilot reaction time due to lower closure rates, all of which contribute to safer carrier operations and thus reduced accident rates.

Summary and Conclusions

The CCW/USB experimental results presented confirm thrust turning through angles up to 165 deg and the associated benefits as a STOL and thrust reverser system, in addition to a potential for VTOL. Application of the test results has led to a proposed conceptual STOL aircraft design to operate from reduced size air-capable ships, possibly without the presence of either catapulting or arresting gear. Results will be refined as additional test data become available and as the proposed aircraft configuration is more adequately defined.

New capabilities are inherent in this CCW + CC/USB high lift system which are not available in existing or proposed high lift systems:

1) Significant improvement in STOL performance is available compared to a conventional flap system (CTOL) on an aircraft with identical weight and thrust; this results from a more than 200% increase in maximum trimmed lift coefficient.

2) Actuators, flaps, and other high lift system moving parts are reduced by nearly 100%.

3) Direct lift control on approach is independent of thrust setting, and is controlled by changes in the bleed air rate supplied to the wing.

4) Higher power setting during approach provides quicker return to maximum thrust for waveoff.

5) Low-speed lateral control is possible by differential wing blowing.

6) A reduced number of parts and reduced impact loads on the aircraft will increase reliability, maintainability, and aircraft lifespan.

7) Vertical landing and eventually vertical takeoff may be feasible with the above advantages (using thrust deflection in the 90-deg range) as improved thrust-to-weight powerplants with lower cruise specific fuel consumption become available.

References

[1] Englar, R.J., Stone, M.B., and Hall, M. "Circulation Control—An Updated Bibliography of DTNSRDC Research and Selected Outside References," DTNSRDC Rept. 77-076, Sept. 1977.

[2] Englar, R.J., Trobaugh, L.A., and Hemmerly, R.A. "STOL Potential of the Circulation Control Wing for High-Performance Aircraft," *Journal of Aircraft*, Vol. 15, March 1978, pp. 175-181.

[3] Englar, R.J., "Development of the A-6/Circulation Control Wing Flight Demonstrator Configuration," DTNSRDC Rept. ASED-79/01, Jan. 1979.

[4] Englar, R.J., Hemmerly, R.A., Moore, W.H., Seredinsky, V., Valckenaere, W.G., and Jackson, J.A., "Design of the Circulation Control Wing STOL Demonstrator Aircraft," AIAA Paper 79-1842, presented at the AIAA Aircraft Systems and Technology Meeting, New York, Aug. 1979.

[5] Pugliese, A.J. and Englar, R.J., "Flight Testing the Circulation Control Wing," AIAA Paper 79-1791, presented at AIAA Aircraft Systems and Technology Meeting, New York, Aug. 1979.

[6] "A-6A Circulation Control Wing Flight Test Final Report," Grumman Aerospace Corp. Rept. FTD-128-55-3.55, April 1979.

[7] Sleeman, W.C. and Hohlweg, W.C., "Low-Speed Wind-Tunnel Investigation of a Four-Engine Upper Surface Blowing Model Having a Swept Wing and Rectangular and D-Shaped Exhaust Nozzles," NASA TN D-8061, Dec. 1975.

[8] Nichols, J.H. Jr., "Development of High Lift Devices for Application to Advanced Navy Aircraft," DTNSRDC Rept. 80/058, April 1980.

[9] McGhee, R.H. and Bingham, G.H., "Low-Speed Aerodynamic Characteristics of a 17-Percent Thick Supercritical Airfoil Section, Including A Comparison Between Wind-Tunnel and Flight Data," NASA TM X-2571, July 1972.

[10] Nichols, J.H. Jr., Englar, R.J., Harris, M.J., and Huson, G.G., "Experimental Development of an Advanced CCW System for Navy STOL Aircraft," AIAA Paper 81-0151, presented at AIAA 19th Aerospace Sciences Meeting, St. Louis Mo., Jan. 1981.

[11] McCracken, R.C., "Quiet Short-Haul Research Aircraft Familiarization Document," NASA Technical Memorandum 81149, Nov. 1979.

[12] Englar, R.J., Trobaugh, L.A., and Hemmerly, R.A., "Development of the Circulation Control Wing to Provide STOL Potential for High Performance Aircraft," AIAA Paper 77-578, presented at the AIAA/NASA Ames V/STOL Conference, Palo Alto, Calif., June 1977.

[13] Turner, T.R., Davenport, E.A., and Riebe, J.M., "Low-Speed Investigation of Blowing from Nacelles Mounted Inboard and on the Upper Surface of an Aspect-Ratio-7.0 35° Swept Wing with Fuselage and Various Tail Arrangements," NASA Memo. 5-1-59L, June 1959.